Charging and Discharging of Oxide Defects in Reliability Issues

Wolfgang Goes, Markus Karner, Viktor Sverdlov, and Tibor Grasser, *Senior Member, IEEE*

***Abstract*—Advances in the microelectronic design implicate a reduction of device dimensions requiring a better understanding of the microscopic processes involved. One of these processes concern charging and discharging of defects via tunneling, which is supposed to constitute a grave contribution to various ongoing reliability issues. A deep understanding and a correct modeling of this mechanism are of utmost importance in this context. Conventionally, tunneling levels are believed to remain at fixed positions within the oxide bandgap regardless whether they are occupied or not. From a theoretical point of view, defect energy levels undergo shifts within the silicon dioxide bandgap after charging or discharging. As a result, defect levels for tunneling into and out of traps have to be distinguished. Based on this understanding of trapping, defects can be characterized as fixed charges, switching oxide charges, interface traps, or other types of defects. In this study, we conduct first-principle investigations on the energetics for a series of individual defects encountered in the context of reliability. In order to deduce their tunneling dynamics, a new model, which accounts for the effects of shifting tunneling levels, has been established. On the basis of the E'_γ center, the main discrepancies between the model relying on trap level shifts and the model with coinciding trap levels have been highlighted.**

***Index Terms*—Charge trapping, fixed charges, interface/oxide states, level shift, structural relaxation.**

I. Introduction

THE EXISTENCE of traps in the dielectrics of semiconductors has been proven by plenty of investigations—in particular, electroparamagnetic-resonance measurements allow the identification of a large number of defects [1], [2]. Several experimental studies indicate electron or hole trapping in $a-\mathrm{SiO_2}$ during bias temperature stress or exposure to irradiation [3], [4]. For instance, Zhang has proposed two types of traps in $\mathrm{SiO_2}$. One is the cycling positive charges (CPCs) which can repeatedly exchange electrons with the interface but their total amount remain unaffected by variations of the temperature. For a switching bias, they give rise to an oscillating behavior in the monitored time evolution of oxide charges. The other defects, the so-called antineutralization positive charges (ANPCs), form a constant background charge which decreases as the temperature is raised. Lelis *et al.* [4] conducted an annealing study on irradiated samples and found an accelerated annealing at elevated temperatures. This phenomenon is traced back to a defect level above the Si conduction band edge so that high energetic electrons are required for the discharging of these defects (also termed switching traps). Other models focusing on reliability issues [5], such as negative bias temperature instability and hot carrier injection, rely on hydrogen reactions at the interface [6] accompanied by the creation of interface states. However, a considerable component of charge trapping has also been supposed to be involved [7] which still requires a fundamental physical proof. The majority of these models rely on defect energies which remain at the same position within the oxide bandgap irrespective of their charge state. However, defect levels are in fact subject to a shift after charging or discharging. The origins are twofold. First, the new charge changes the Coulomb forces that determine the position of the energy levels. Second, the atoms proximate to the defect undergo a structural relaxation accompanied by strengthening, weakening, or even disrupting bonds. According to the Franck–Condon principle [8], this shift of energy levels occurs within femtoseconds compared to the considerably larger time constants observed for tunneling. In other words, the atomic configuration will adopt the new charge state before a new tunneling process can change the charge state of this defect again. This concept of charging and discharging has not received much attention to date, but has important implications on the tunneling kinetics in $a-\mathrm{SiO_2}$ as will be shown in the following.

The remainder of this paper is divided into two parts. The first addresses the evaluation of trap levels for a series of defects and is organized as follows. Section II summarizes the employed methods and their technicalities used throughout this study, while the successive Sections III–VI show detailed results for the individual defects. Additionally, a classification of these defects has been carried out. In the second part, Sections VII and VIII, the discrepancies in the temporal trapping behavior which emerge through trap level shifts are discussed.

II. Method

The issue of defect levels can be tackled within the framework of first-principle simulations. Theoretical investigations based on a more detailed understanding of trapping have already been undertaken using a crystalline structure for silicon dioxide $(c-\mathrm{SiO_2})$ [9]–[11]. At this point, we want to stress the fact that it is necessary to take the amorphous nature of silicon dioxide $(a-\mathrm{SiO_2})$ into account. As highlighted in [12]

Manuscript received December 30, 2007; revised March 20, 2008. First published September 9, 2008; current version published October 16, 2008.

W. Goes and T. Grasser are with the Christian Doppler Laboratory for TCAD in Microelectronics, Institute for Microelectronics, Technische Universität Wien, 1040 Wien, Austria.

M. Karner is with the Christian Doppler Laboratory for TCAD in Microelectronics, Institute for Microelectronics, Technische Universität Wien, 1040 Wien, Austria, and also with Global TCAD Solutions, 1030 Vienna, Austria.

V. Sverdlov is with the Institute for Microelectronics, Technische Universität Wien, 1040 Wien, Austria.

Color versions of one or more of the figures in this paper are available online at http://ieeexplore.ieee.org.

Digital Object Identifier 10.1109/TDMR.2008.2005247

1530-4388/$25.00 © 2008 IEEE

Authorized licensed use limited to: Universitatsbibliothek der TU Wien. Downloaded on December 9, 2008 at 08:13 from IEEE Xplore. Restrictions apply.

TABLE I
COMPARISON OF THE CHARACTERISTIC PROPERTIES OF THE PRODUCED $a-SiO_2$. d_{Si-O}, d_{O-O}, AND d_{Si-Si} DENOTE THE FIRST MAXIMA IN THE APPROPRIATE PAIR-CORRELATION FUNCTION. $\phi_{Ox-Si-Ox}$ AND $\phi_{Si-Ox-Si}$ GIVE THE MAXIMUM OF THE APPROPRIATE ANGLE DISTRIBUTION IN EXCELLENT AGREEMENT WITH PUBLISHED VALUES [16]–[18]

	d_{Si-O}	d_{O-O}	d_{Si-Si}	$\phi_{Ox-Si-Ox}$	$\phi_{Si-Ox-Si}$
Here	1.64	2.66	3.08	109.42	142.62
[16]	1.62	2.64	3.10	109.6	142.0
[17]	1.63	2.67	3.11	109.4	146.8
[18]	1.62	2.68	2.98	109	136

TABLE II
ENERGY TRAP LEVELS ($+/0$, $0/+$, ETC.) RELATIVE TO THE THEORETICAL OXIDE VALENCE BAND MAXIMUM OF $a-SiO_2$. THE FIRST SIGN DENOTES THE EQUILIBRIUM CONFIGURATION OF THE DEFECT IN THE CORRESPONDING CHARGE STATE, AND THE SECOND SIGN GIVES THE CHARGE STATE OF THE DEFECT FOR A GIVEN CONFIGURATION

	E'_δ	E'_γ	E'_δH	H
$+/0$	$1.7-3.6$ eV	$3.9-4.1$ eV	$4.4-4.9$ eV	$4.9-5.1$ eV
$0/+$	$0.3-0.5$ eV	$2.1-2.4$ eV	$1.7-2.3$ eV	$0.3-0.9$ eV
$0/-$			$4.1-4.3$ eV	$3.2-4.4$ eV
$-/0$			$1.2-2.6$ eV	$0.9-1.2$ eV

and [13], crystalline structures used in theoretical examinations do not succeed in reproducing the properties of silicon dioxide in a satisfactory manner. Convincing support of this argument is provided through investigations on thermal oxidation. O_2 molecules encounter a spread of barriers to migrate from one void to the next in amorphous silicon dioxide. This distribution of barriers determines the activation energy for the diffusion process [14]. In contrast to that, O_2 molecules have only single-valued barriers to overcome in a crystalline structure. The need to mimic the oxide with $a-SiO_2$ is also supported by the stability of the E'_γ center depending on the local surrounding silica network [13]. In the following, we give an overview of the simulation approach used to obtain defect energy levels. The method of choice regarding the evaluation of defect levels is the density functional theory (DFT). To reduce the computational costs, an empirical potential molecular dynamical (MD) approach has been employed for the production of $a-SiO_2$. The Si and O atoms are placed randomly within the simulation cell respecting exclusion radii as to avoid any overlap between the atoms. The size of the simulation cell (11.79 Å) has been chosen to exactly match the mass density (2.19 g/cm^3) observed experimentally. Taking this random structure as a starting configuration, the amorphous structure is allowed to evolve at high temperatures using an MD approach (BKS potential) [15]–[18]. The MD simulations comprise of an equilibration step at 3000 K for 30 ps with a timestep of 1 fs which was followed by a quenching step to 0 K for 30 ps with a timestep of 1 fs. To prepare the amorphous samples for subsequent first-principle calculations, structural minimization, based on DFT simulations with the same exchange-correlation potential as used later again, has been performed. Since edge-sharing tetrahedra are unfavored from an energetic point of view, samples containing these edge-sharing tetrahedra are excluded from further investigations. The remaining samples exhibit no miscoordination. Pair-correlation functions, angle distributions, and the ring distribution have been evaluated, to make sure that the obtained samples correspond to $a-SiO_2$. Perfect agreement has been achieved with previously published results [16]–[18] (see Table I). The exchange-correlation kernel used in our DFT calculations (VASP [19]–[23]) is based on gradient corrections, and the projector augmented wave method is used to represent ion cores. The plane wave cutoff energy was set to 400 eV. Structural optimization was achieved through a conjugate gradient algorithm which limits the force on each atom to be below 0.3 eV/Å. Charged supercells were calculated, introducing a homogeneous compensating background charge to ensure neutrality within the supercell. The use of a plane wave code implicitly involves periodic boundary conditions and implies interactions between periodically arranged defects. To minimize this effect, large supercells of $a-SiO_2$ ($\sim$11.79 Å) comprising of 36 SiO_2 units (108 atoms) were chosen. The integration of the Brillouin zone is constricted to the Γ point only. Defect levels for tunneling mechanisms (also referred to as switching levels or transition states) are calculated as the energy difference between two differently charged supercells. The atomic structure is kept fixed pertaining to the Franck–Condon principle.

$$\varepsilon^{+/0}[X^+] = E_f^0[X^+] - E_f^+[X^+] \quad (1)$$

$$\varepsilon^{0/+}[X^0] = E_f^0[X^0] - E_f^+[X^0] \quad (2)$$

$$\varepsilon^{-/0}[X^-] = E_f^-[X^-] - E_f^0[X^-] \quad (3)$$

$$\varepsilon^{0/-}[X^0] = E_f^-[X^0] - E_f^0[X^0] \quad (4)$$

The sign in E_f^q corresponds to the formation energy in the charge state q, where $[X^q]$ denotes the equilibrium configuration. For the sake of clarity, the $\varepsilon^{+/0}$ energy level comes into play for positive defects (X^+) which should be neutralized. The $\varepsilon^{0/+}$ energy level applies to the inverse process when neutral defects (X^0) capture positive charge carriers. Analogous considerations hold true for the energy levels $\varepsilon^{-/0}$ and $\varepsilon^{0/-}$. Concerning the bandgap alignment, we used the procedure proposed in [9]. However, due to the amorphous nature of SiO_2, we found a valence band offset of approximately 2.6 eV consistent with valence band offsets extracted from [24] and [25]. Although a similar study on trap-assisted tunneling in $c-SiO_2$ has been conducted [9], the impact of the amorphous nature of silicon dioxide on the tunneling levels has not been investigated up to date. The focus of this paper is placed on reexamining trap levels in an amorphous silica network. Based on the knowledge of the position of the defect levels (listed in Table II) within the silicon dioxide bandgap, a list of defects, suspected to be charged oxide traps in MOSFET structures, will be discussed.

III. O VACANCY

In stoichiometric $a-SiO_2$, Si atoms are connected via bridging O atoms. As shown in Fig. 1, an oxygen vacancy (V_O) can be pictured by the removal of a bridging O atom. The remaining dangling bonds originating from the neighboring Si atoms form a common bond of the typical bond length observed in silicon bulk. This bond (see Fig. 2) is associated with a trap level far below the silicon conduction band edge. The positively charged counterpart of the O vacancy is referred to as

Authorized licensed use limited to: Universitatsbibliothek der TU Wien. Downloaded on December 9, 2008 at 08:13 from IEEE Xplore. Restrictions apply.

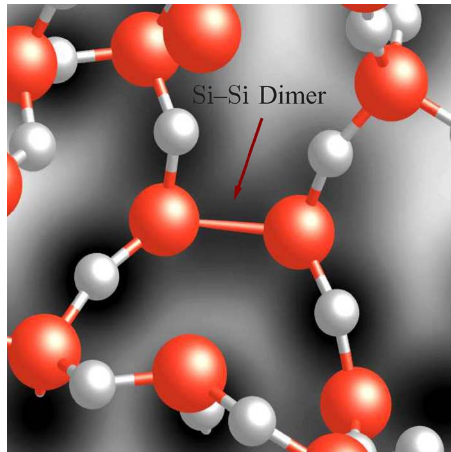

Fig. 1. Electron density plot of an oxygen vacancy. The reestablished Si–Si bond is indicated by a high charge density between the neighboring Si atoms. [(Dark area) high density, (white area) low density, (big dark spheres) Si atoms, and (small light spheres) O atoms].

the E'_δ center. The removal of one electron causes a repulsion between both Si atoms, accompanied by a strong increase of the Si–Si bond length. However, the common bond still persists, giving rise to one defect level close to the silicon valence band edge. This bond experiences a strongly varying tensile force due to the amorphous nature of silicon dioxide which explains the wide spread of $0/+$ energy levels for the E'_δ center. For the O vacancy, the impact of the surrounding network can be neglected compared to the strength of the Si–Si bond. Concerning the tunneling dynamics, one has to differentiate between two cases: If the defect level $+/0$ is located below the silicon valence band edge, electrons residing in the substrate will tunnel into the defect. Therefore, a tunneling process of an electron from the silicon valence band into the singly occupied defect state is allowed. For the reverse process, the defect level is already shifted downward. From here, the electron is unlikely to find a high energetic h^+ from the substrate. In short, this defect remains neutral if it is discharged once. In the case that the defect level $+/0$ is located above the silicon valence band edge, the neutralization of the defect via interaction with the conduction band states is impeded. These charges, however, will be neutralized via interface states instead.

IV. E'_γ CENTER AND VARIANTS

The existence of the E'_γ center, a stable partner of the E'_δ center, has been confirmed by a wide range of both theoretical [12], [13] as well as experimental [26] studies. Starting from the E'_δ center, one side of this defect undergoes the well-established puckering. There, the Si atom emerging from the disruption of the Si–Si dimer moves through the plane defined by its three O neighbors. This new configuration is stabilized via a weak bond of a Si atom to a further nearby bridging O atom. On the other side of this defect, an unpaired electron in a dangling bond is left behind. The respective configuration is shown in Fig. 3. In contrast to the O vacancy, the E'_γ center exhibits only a small spread in its defect levels because the dangling bond on the left-hand side of Fig. 3 undergoes only little relaxation. The puckered side of the defect complex does not interfere

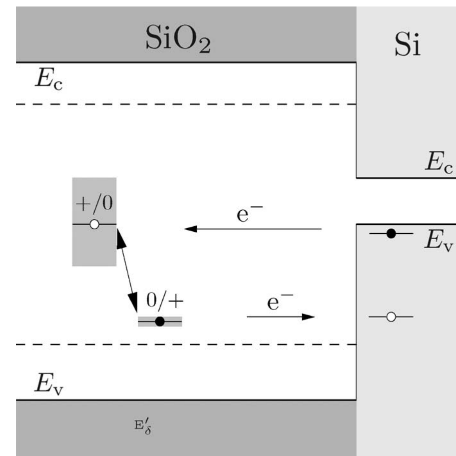

Fig. 2. Schematic of defect levels arising from O vacancies or E'_δ centers, respectively. The $+/0$ levels ($\varepsilon_{+/0}$) are related to the capture of electrons. The $0/+$ levels ($\varepsilon_{0/+}$) apply to the inverse process, the emission of electrons. The arrow represents the Franck–Condon shift of energy levels, and the spread of energy levels is indicated by the gray box. The wide spread of $\varepsilon_{+/0}$ levels requires a distinction whether the $\varepsilon_{+/0}$ levels lies above or below the silicon valence band edge.

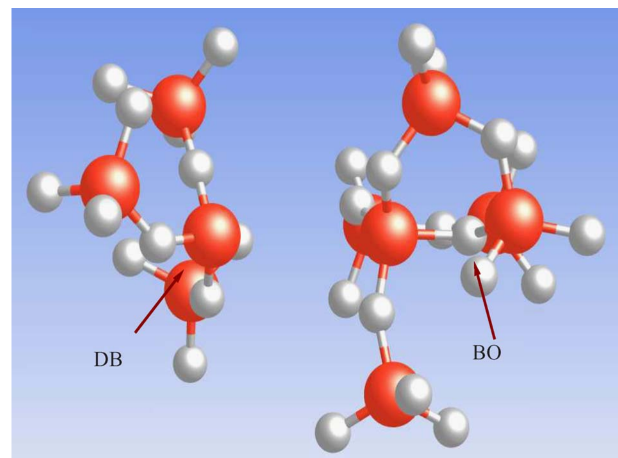

Fig. 3. Structure of an E'_γ center. The silicon atom on the left-hand side carries (DB) an electron in the dangling bond. The positively charged silicon atom on the right-hand side is bonded to (BO) the back oxygen. This atomic arrangement is also referred to as the puckered configuration.

with the dangling bond and, in consequence, does not affect its energetics. The levels for tunneling into $(+/0)$ or out of $(0/+)$ the traps lie close to the respective silicon band edges (see Fig. 4). Thus, only a small thermal excitation of charge carriers in the substrate is required for a tunneling process between the substrate and the defect. In this case, the band bending governs the concentrations of electrons in the silicon conduction band or holes in the silicon valence band, respectively, and, in consequence, controls the corresponding tunneling rates. In conclusion, the E'_γ defect is a good candidate for CPCs which are capable of repeatedly exchanging electrons with the channel in MOSFETs [27]. Moreover, this defect configuration was already proposed by Lelis [28] for the temperature-dependent annealing behavior of traps in silicon dioxide. The temperature dependence in his model is related to a spin-triplet [4] state which can capture electrons from the substrate by tunneling. At elevated temperatures, the concentration of excited

Authorized licensed use limited to: Universitatsbibliothek der TU Wien. Downloaded on December 9, 2008 at 08:13 from IEEE Xplore. Restrictions apply.

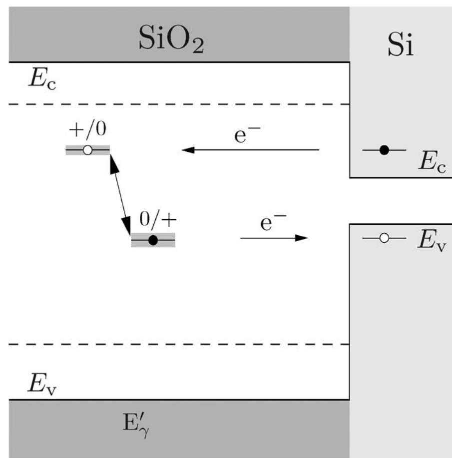

Fig. 4. Schematic of the defect levels originating from an E'_γ center. The energy levels for the capture of electrons $(+/0)$ as well as the energy levels for the emission of electrons $(0/+)$ are found to lie close to the silicon conduction band or the silicon valence band, respectively.

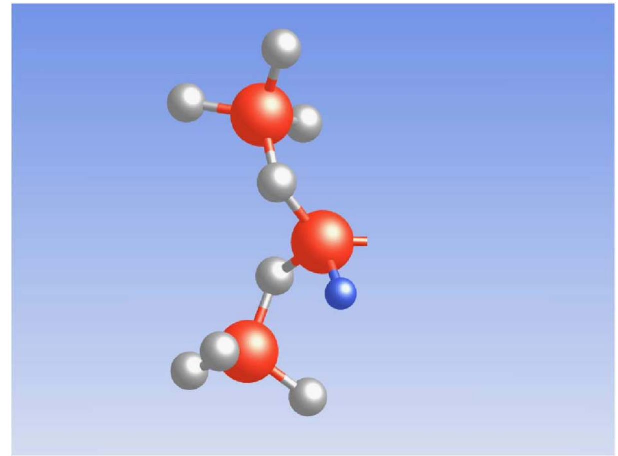

Fig. 5. Representation of an E'_{74} center. One of the neighboring O atoms is replaced by an H atom which shows a tendency to bond to a silica network atom. [(Big dark spheres) Si atoms, (small light spheres) O atoms, and (small dark spheres) H atoms].

electrons which are capable of undergoing a tunneling process is increased. As a result, the annealing of positively charged defects is accelerated. The proposed trap level [4] in the Lelis model, namely, the spin-triplet state, coincides with the defect level for neutralization in the present study. The defect levels leading to the annealing behavior in the Lelis model have been theoretically confirmed but an alternative interpretation has been given. As highlighted in [13], a fraction of E'_γ centers in $a - \mathrm{SiO_2}$ (termed $E'_{\gamma 5}$ centers) collapses into the so-called dimer configuration after neutralization. The final structure coincides with that of an O vacancy. Identically to the situation of the E'_γ centers, the defect level starts at the same position above the silicon conduction band. However, after neutralization, the respective energy level shifts down far below the silicon valence band edge as in the case of the O vacancy. Therefore, once this defect is neutralized, it cannot be recharged again and will be annealed out permanently. However, this does not rule out the E'_γ center as a cycling charge since a considerable fraction of E'_γ centers may remain in the puckered configuration when neutralized. In this configuration, they are capable of repeatedly exchanging electrons or holes, respectively with the interface. Another variant of the E'_γ center is the E'_{74} center (shown in Fig. 5) which has been extensively examined by Conley and Lenahan [26]. Its structure can be imagined by replacing one of the nearby O atoms with an H atom. Calculations on this defect show that the neighboring H atom does not affect the position of the defect levels originating from the dangling bond. As a result, this defect can perhaps be categorized as a switching trap or a CPC. However, mind that, in many cases, a bond between the H atom and another network atom could be observed, giving rise to different defect levels related to a different trapping behavior.

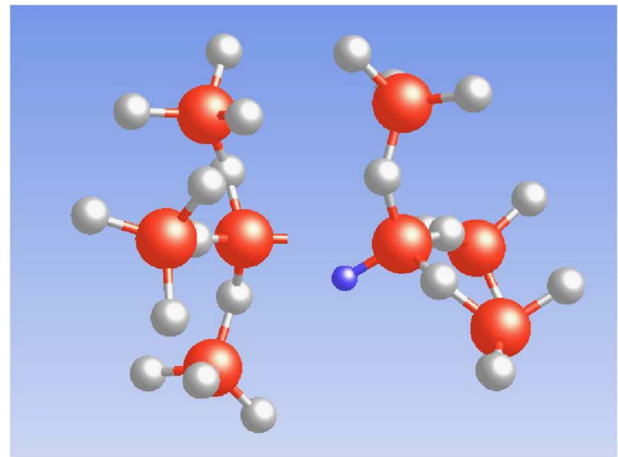

Fig. 6. Representation of the H bridge in the neutral charge state. For the positively charged defect, there arises a Si–H–Si bond chain. After neutralization, this chain is disrupted, yielding a dangling bond on the left-hand side of this complex and a saturated dangling bond on the right-hand side. In the case of a negatively charged H bridge, the Si–H bond is bent away from the dangling bond.

V. H BRIDGE

In addition, we examined a hydrogenated variant of the E'_δ center, which is also referred to as the H bridge (see Fig. 6). In this case, the H atom places itself between both adjacent Si atoms of the E'_δ center. The H atom of this complex exhibits a symmetry in distances to both Si atoms, whereas this symmetry is broken in the neutral case. Therefore, much structural relaxation is undergone which, in turn, explains the wide spread in defect energy levels. All defect levels (Fig. 7) are located within reasonable distance from silicon band edges in the energy scale. Therefore, all transitions between the substrate and the defect are allowed, and therefore, this defect will appear in all charged variants. As for the E'_γ center, the charge state of this defect depends on the band bending of the substrate. In summary, this defect can be classified as an interfacelike trap exhibiting large time constants.

VI. H ATOM

In the context of reliability issues, the H atom is of special interest, because it is available in appreciable amounts and should be investigated as a possible candidate for trapped charges. Many investigations have shown that hydrogen is indeed a

Authorized licensed use limited to: Universitatsbibliothek der TU Wien. Downloaded on December 9, 2008 at 08:13 from IEEE Xplore. Restrictions apply.

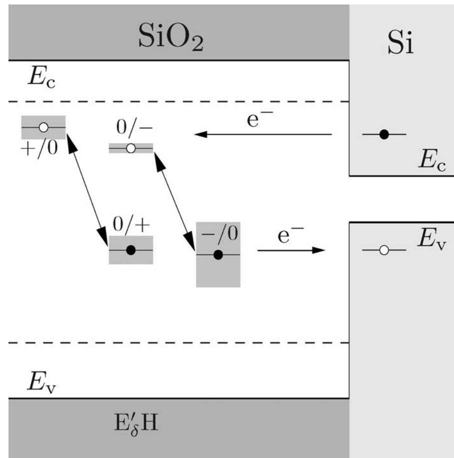

Fig. 7. Schematic of defect levels of an H bridge. All energy levels are located within an appropriate distance in the energy scale and allow an exchange of charge carriers in timescales of interest.

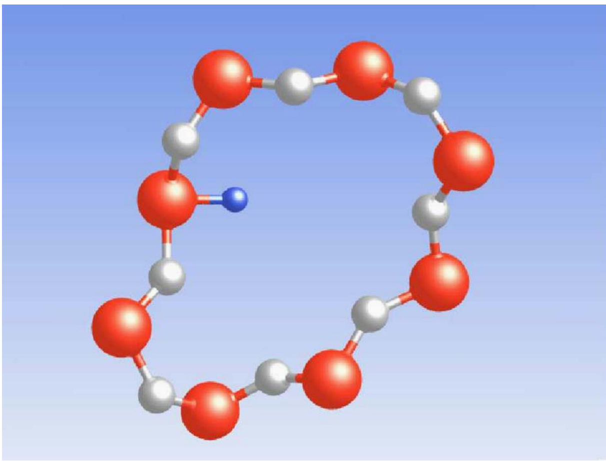

Fig. 8. Representation of a proton attached to the silica network. The H^+ attaches to the bridging O atom, the H^0 is situated in the middle of a void, and the H^- forms a weak bond to a network Si atom.

prime suspect in reliability issues. Its configuration strongly differs with its charge state: The neutral H^0 atom resides in the middle of a void. The positive H^+ atom loosely binds to network O atoms (shown in Fig. 8), and the negative H^- atom attaches itself to network Si atoms. However, the energy levels of this defect are located too far away from the silicon band edges so that exchanging electrons with the interface is impeded. The sole exception is the trap level $0/-$ for charging the hydrogen atom negatively. That is to say that charged H atoms keep their charge state. For the neutral H atom, the data in Fig. 9 suggest that the H atom slightly tends to take the negative charge state. At a first glance, this contradicts the findings of other groups [29]–[31] concerning the most stable charge state of the H atom being the proton. However, these calculations are based on a fast exchange of e^- between defects within the silicon oxide. These interactions are supposed to occur at large timescales compared to charging or discharging, respectively, and should therefore play a minor role. For pMOSFETs, the silicon band edge is bent down associated with a decreasing density of electrons near the interface. Therefore, a transition of an electron from the silicon into a defect becomes less likely.

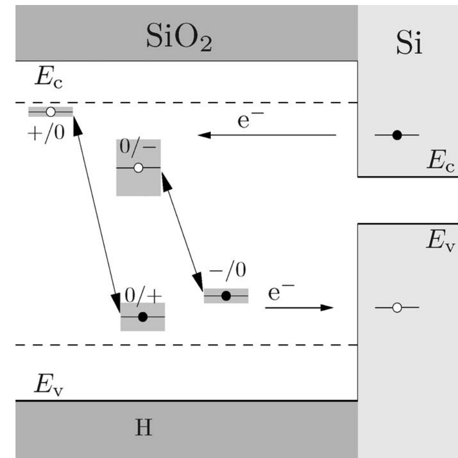

Fig. 9. Schematic of defect levels of the H atom. The energy levels for charging and discharging are far away from the respective silicon band edges. Only the energy levels $0/-$ for charging the H^0 positively allow transition rates in a magnitude of interest.

VII. Modeling of Trapping and Detrapping

From the theoretical point of view, the rate equation

$$\frac{\partial n_t}{\partial t} = \tilde{r}_{\mathrm{in}} - \tilde{r}_{\mathrm{out}} \tag{5}$$

combined with Fermi's golden rule

$$\tilde{r}_{\mathrm{in/out}} = \sum_\alpha \sum_\beta \frac{2\pi}{\hbar} |M_{\alpha,\beta}|^2 \delta(E_\alpha - E_\beta) \Big|_{E_\beta = E_{\mathrm{in/out}}} \tag{6}$$

forms the basis for a proper description of charge trapping. The following description of trapping and detrapping is based on the approach of Tewsbury [32] including some slight modifications. The subscript α denotes the initial states, whereas the β stands for the final states. The summation over the initial states accounts for the number of charge carriers which are decomposed in an electronic density of states and their respective occupancies. The final states corresponds to the number of unoccupied trap states n_t which are expressed by a trap density ρ_t and its occupancy f_t. The calculation of the matrix element $M_{\alpha,\beta}$ is restricted to one dimension but is corrected by introducing a capture cross section σ according to Freeman and Dahlke's approach [33]. The capture cross section is identified by a comparison to a 3-D model [32] which avoids any arbitrary fitting parameters. The incorporation of trap level shifts is achieved by evaluating the individual trap rates for tunneling into and out of traps at E_{in} and E_{out}, respectively. Note that charging and discharging via interface states, which can play an important role [32] but are basically analogous processes, are neglected here. In order to establish the basic properties of our approach, we assume traps with two charge states only. This implies that only two rates participate in charge trapping, namely, $r_{\mathrm{in}}(E_{\mathrm{in}})$ and $r_{\mathrm{out}}(E_{\mathrm{out}})$. Covering for both, we end up in

$$\frac{\partial f_t}{\partial t} = n(E_{\mathrm{in}}) \cdot r_{\mathrm{in}}(E_{\mathrm{in}}) \cdot (1 - f_t) - p(E_{\mathrm{out}}) \cdot r_{\mathrm{out}}(E_{\mathrm{out}}) \cdot f_t \tag{7}$$

Authorized licensed use limited to: Universitatsbibliothek der TU Wien. Downloaded on December 9, 2008 at 08:13 from IEEE Xplore. Restrictions apply.

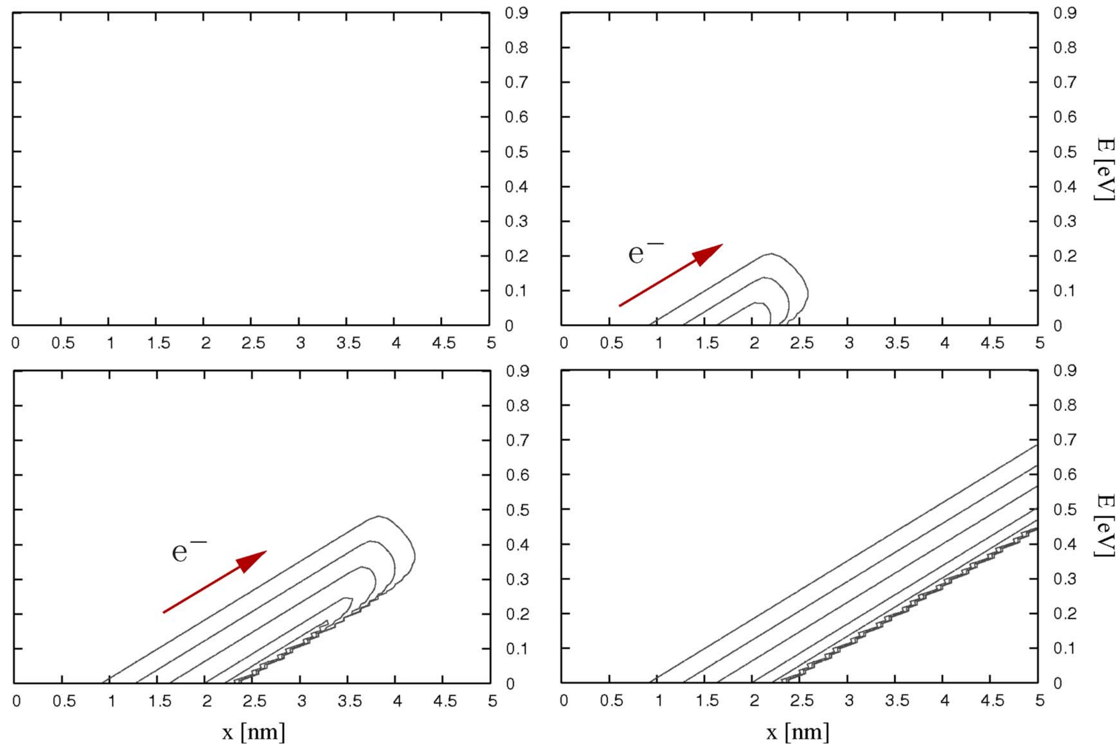

Fig. 10. Fixed level model depicted at four different times during the stress/trapping phase. The contour plots represent trap occupancies pertaining to trap levels distributed in energy and real space. The y-axis shows the trap level $\varepsilon_{+/0}$ measured from the silicon conduction band edge. Note that the trap level $\varepsilon_{+/0}$ shifts below the silicon valence band down to $\varepsilon_{0/+}$ after being occupied. The x-axis gives the distance from the interface. Mind that the applied electric field is reflected in a spatial incline of the oxide band edge energy. (Top left) In depletion, the silicon dioxide is swept out of e$^-$. (Top right) When the substrate is forced to inversion, traps situated slightly above the silicon conduction band edge capture e$^-$ from the substrate. (Bottom left) As the time proceeds, e$^-$ fill up traps residing more distant from the interface. (Bottom right) At the end of the trapping phase, all trap levels slightly above the silicon conduction band are occupied.

where n and p denote the electron and hole concentrations at the interface, respectively. Note that tunneling from the silicon conduction band into a defect state is assumed to be an elastic process. In between trapping and detrapping events, the defect undergoes structural relaxation and releases energy accompanied by a shift of the respective trap level. In the following, the conventional model based on coinciding levels for tunneling into and out of traps is termed fixed level model, whereas the model relying on level shifts is referred to as level shift model. For the case of the fixed level model, the rates are evaluated for $E_{\mathrm{in}} \sim E_{\mathrm{out}}$ in (7).

VIII. Effect of Level Shifts

Numerical investigations have been performed to study the differences between the level shift model and the fixed level model. For this purpose, the E'_γ center has been chosen which features $+/0$ trap levels approximately 0.8 eV above the silicon conduction band edge and $0/+$ trap levels approximately 0.3 eV below the silicon valence band edge. The respective trap levels are distributed uniformly in space, while the energetical spread of trap levels is assumed to take a Gaussian shape with the square root of the variance set to 0.15 eV (see Table II). Numerical simulations of the rate equation [(7)] have been performed at 300 K and rely on self-consistent band edge energy calculations for a 5-nm-thick n-channel MOSFET supplied by the Vienna Schrödinger–Poisson solver [34]. Initial trap occupancies according to steady state conditions are obtained by preceding calculations based on sufficiently long time spans. For the fixed level model, the $\varepsilon_{0/+}$ level is assumed to coincide with the $\varepsilon_{+/0}$ level.

The time evolution of the trap occupancy for the fixed level model is shown in Figs. 10 and 11. Due to the balance between trapping and detrapping, trap levels in an energy range slightly above the Fermi energy are filled by e$^-$. At higher energy levels, detrapping is favored, giving rise to a negligible trap occupancy there. The balance between rates is not affected by the depth of traps but the rates themselves show an exponential decay with increasing distance from the interface. As a consequence, traps near the interface achieve equilibrium at first, correlating with a saturation in their local occupancies. Then, temporal filling of traps continues from near to the interface to deep into the dielectric, as shown in Fig. 10. Similar considerations hold true for detrapping as shown in Fig. 11. There, the emission of e$^-$ starts near the interface and proceeds deep into the silicon dioxide.

According to the level shift model (see Figs. 12 and 13), the trapping rate dominates over the detrapping rate—even when no voltage is applied to the gate. This originates from the large valence band offset which implies high tunneling barriers for h$^+$ to overcome and impedes tunneling out of traps. Only in a small band with trap levels just below the silicon valence band edge, the high h$^+$ concentration induces a high detrapping rate which outbalances the trapping rate and

Authorized licensed use limited to: Universitatsbibliothek der TU Wien. Downloaded on December 9, 2008 at 08:13 from IEEE Xplore. Restrictions apply.

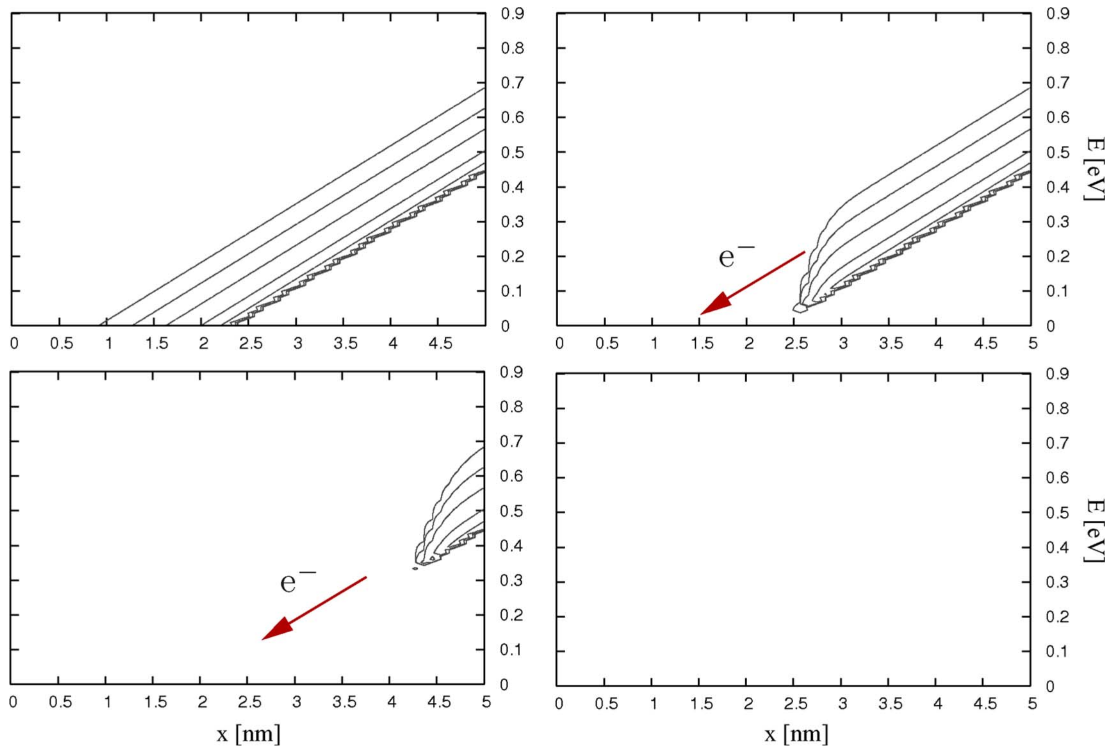

Fig. 11. Fixed level model depicted at four different times during the recovery/detrapping phase. (Top left) After the trapping phase, trap levels slightly above the silicon conduction band edge are occupied by e^-. (Top right) When the gate bias is removed, detrapping is favored and trap states near the interface are emptied at first. (Bottom left and right) This process continues until the oxide is completely swept out of e^-.

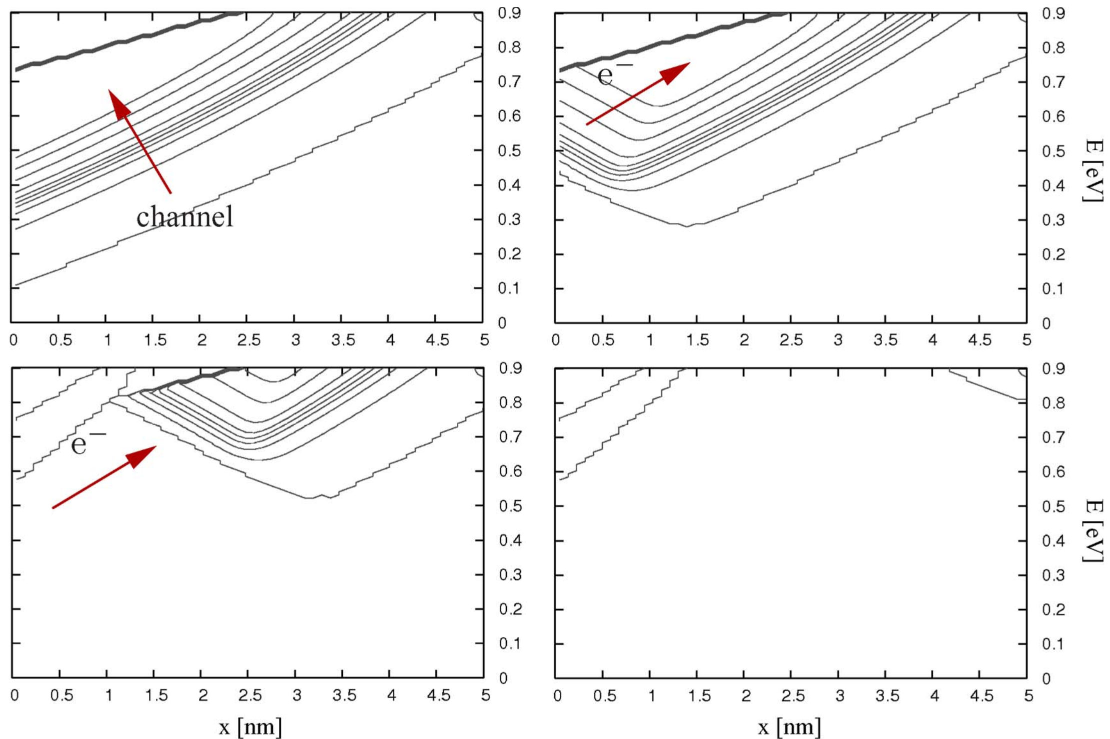

Fig. 12. Level shift model depicted at four different times during the stress/trapping phase. (Top left) As equilibrium prevails, all trap states are filled—except for a small band of trap levels which are located slightly below the silicon valence band. (Top right and bottom left) As the applied gate bias forces the substrate into inversion, trapping into the remaining free trap states sets in (as indicated by the red arrow). (Bottom right) This figure illustrates that all trap levels are fully occupied by e^- at the end of the stress phase.

Authorized licensed use limited to: Universitatsbibliothek der TU Wien. Downloaded on December 9, 2008 at 08:13 from IEEE Xplore. Restrictions apply.

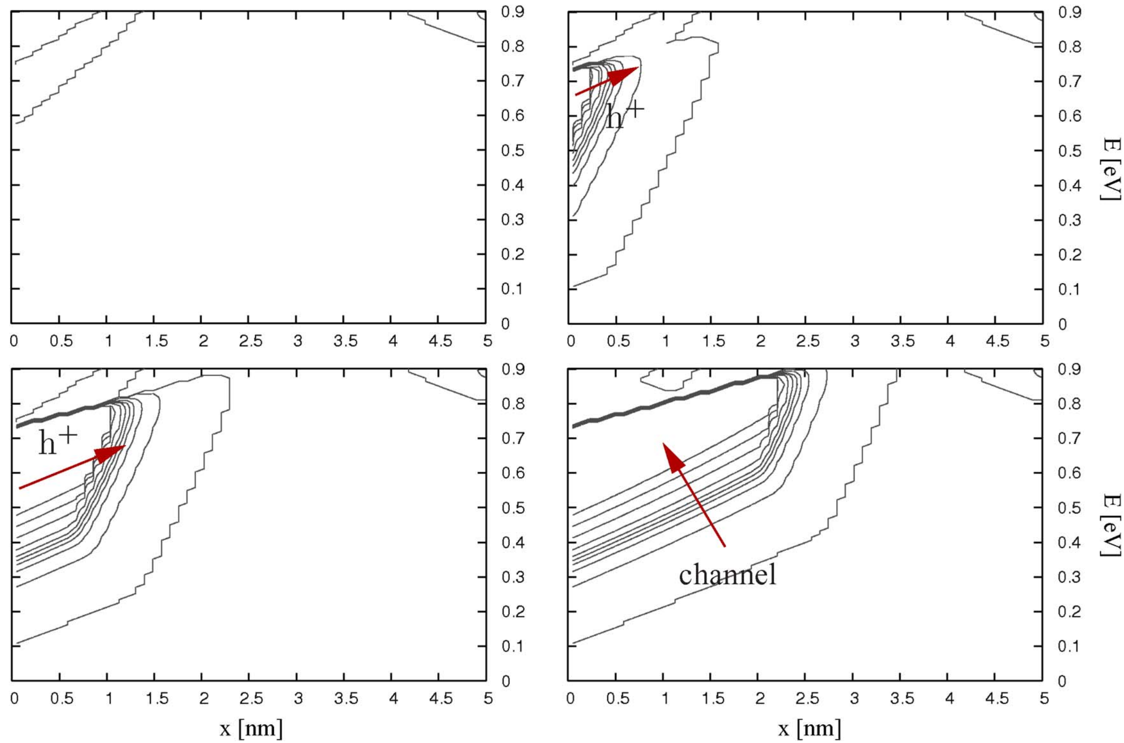

Fig. 13. Level shift model depicted at four different times during the recovery/detrapping phase. (Top left) Before the gate bias is removed, all oxide traps are completely filled up by e^-. (Top right and bottom left and right) During the relaxation phase, the same band of unoccupied trap states as in Fig. 12 is rebuilt again.

empties these trap levels in return. As a voltage is applied to the gate, the detrapping rate is suppressed and the aforementioned band vanishes. Returning to the initial conditions, the channel rebuilds again.

In the following, the impact of trapping according to the fixed level model and the level shift model is studied. The threshold voltage shift governed by the trap occupancy can be calculated making use of

$$\Delta V_{\mathrm{th}}(t) = \frac{q_0}{C_{\mathrm{ox}}} \int_{0}^{t_{\mathrm{ox}}} \int_{E_{t,\mathrm{min}}}^{E_{t,\mathrm{max}}} \left(1 - \frac{x}{t_{\mathrm{ox}}}\right) \rho_t \Delta f_t(E_t, x, t) dE_t dt \tag{8}$$

where C_{ox} denotes the silicon dioxide capacitance. The integration runs over the oxide thickness and the range of trap levels in order to account for all traps within the silicon oxide. The charging–discharging cycle, shown in Fig. 14, demonstrates the difference between the fixed level model and the level shift model. During the stress phase, a fast increase in the threshold voltage according to the level shift model can be observed compared to the fixed level model (see Fig. 15). Discharging during the recovery phase, however, occurs on much larger timescales than in the fixed level model (see Fig. 16). This behavior can be traced back to different orders of magnitude in detrapping rates. According to the level shift model, detrapping is nearly suppressed since the high barrier of the valence band impedes tunneling out of traps. In the fixed level model, however, the captured e^- escape through the conduction band, where a huge number of unoccupied states exist. This involves high detrapping rates, which entails a slower charging but much faster discharging behavior. As a result, charging, according to the level shift model, is accelerated, while discharging is diminished compared to the fixed level model.

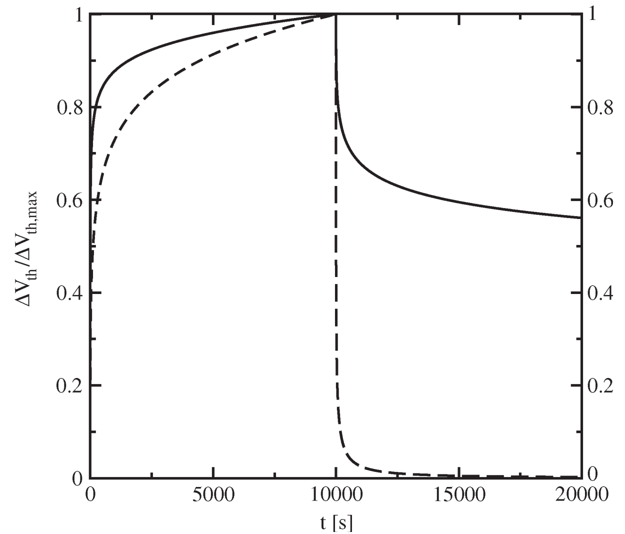

Fig. 14. Comparison between the (solid line) level shift model and the (dashed line) fixed level model. For 10 000 s, the device is forced to inversion followed by 10 000 s where the device is operated in depletion.

IX. Conclusion

We have carried out an investigation of trapping and detrapping energy levels. For example, the E'_γ center should be considered as a defect capable of exchanging electrons with the interface, while an O vacancy is found to remain neutral.

Authorized licensed use limited to: Universitatsbibliothek der TU Wien. Downloaded on December 9, 2008 at 08:13 from IEEE Xplore. Restrictions apply.

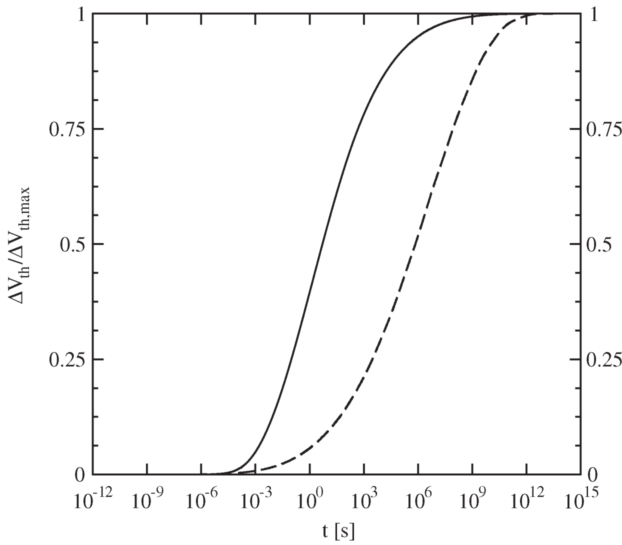

Fig. 15. Normalized ΔV_{th} transient according to the (solid line) level shift model compared to the (dashed line) fixed level model for the nMOSFET operated in inversion.

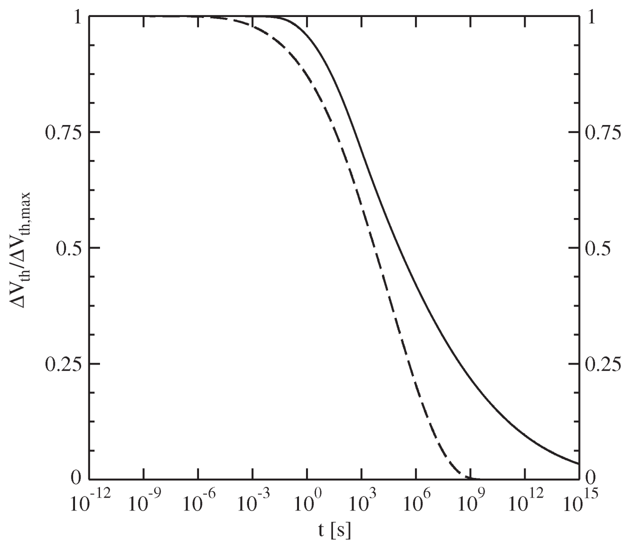

Fig. 16. Normalized ΔV_{th} transient according to the (solid line) level shift model compared to the (dashed line) fixed level model for the nMOSFET operated in depletion.

The H bridge can be classified as an interfacelike trap with large time constants. For the H atom, any trapping or detrapping mechanism is impeded except from charging the neutral H atom negatively. For a proper description of the physics underlying trapping and detrapping mechanisms, it is of utmost importance to incorporate trap level shifts. Simulations concerning the E'_γ center clearly demonstrate a pronounced increase in the threshold voltage shift compared to the fixed level model for an applied gate bias. For no bias on the gate, the decay of the threshold voltage shift extends over long timescales.

ACKNOWLEDGMENT

The authors would like to thank S. T. Pantelides, I. G. Batyrev, F. Mittendorfer, and G. Kresse for the helpful discussions and comments.

REFERENCES

[1] P. M. Lenahan and J. F. Conley, "What can electron paramagnetic resonance tell us about the Si/SiO_2 system?" *J. Vac. Sci. Technol. B, Microelectron. Process. Phenom.* vol. 16, no. 4, pp. 2134–2153, Jul. 1998.

[2] E. H. Poindexter and W. L. Warren, "Paramagnetic point defects in amorphous thin films of SiO_2 and Si_3N_4: Updates and additions," *J. Electrochem. Soc.*, vol. 142, no. 7, pp. 2508–2516, Jul. 1995.

[3] D. M. Fleetwood, H. D. Xiong, Z.-Y. Lu, C. J. Nicklaw, J. A. Felix, R. D. Schrimpf, and S. T. Pantelides, "Unified model of hole trapping, 1/f noise, and thermally stimulated current in MOS devices," *IEEE Trans. Nucl. Sci.*, vol. 49, no. 6, pp. 2674–2683, Dec. 2002.

[4] A. J. Lelis, T. R. Oldham, H. E. Boesch, and F. B. McLean, "The nature of the trapped hole annealing process," *IEEE Trans. Nucl. Sci.*, vol. 36, no. 6, pp. 1808–1815, Dec. 1989.

[5] V. Huard, M. Denais, F. Perrier, N. Revil, C. Parthasarathy, A. Bravaix, and E. Vincent, "A thorough investigation of MOSFETs NBTI degradation," *Microelectron. Reliab.*, vol. 45, no. 1, pp. 83–98, Jan. 2005.

[6] L. Tsetseris, X. J. Zhou, D. M. Fleetwood, R. D. Schrimpf, and S. T. Pantelides, "Hydrogen-related instabilities in MOS devices under bias temperature stress," *IEEE Trans. Device Mater. Rel.*, vol. 7, no. 4, pp. 502–508, Dec. 2007.

[7] V. Huard, C. Parthasarathy, N. Rallet, C. Guerin, M. Mammase, D. Barge, and C. Ouvrard, "New characterization and modeling approach for NBTI degradation from transistor to product level," in *IEDM Tech. Dig.*, 2007, pp. 797–800.

[8] T. Bakos, S. N. Rashkeev, and S. T. Pantelides, "Role of electronic versus atomic relaxations in stokes shifts at defects in solids," *Phys. Rev. Lett.*, vol. 91, no. 22, p. 226 402, Nov. 2003.

[9] P. E. Blöchl, "Aspects of defects in silica related to dielectric breakdown of gate oxides in MOSFETs," *Phys., B Condens. Matter*, vol. 273/274, pp. 1022–1026, Dec. 1999.

[10] P. E. Blöchl and J. H. Stathis, "Hydrogen electrochemistry and stress-induced leakage current in silica," *Phys. Rev. Lett.*, vol. 83, no. 2, pp. 372–375, Jul. 1999.

[11] P. E. Blöchl, "First-principles calculations of defects in oxygen-deficient silica exposed to hydrogen," *Phys. Rev. B, Condens. Matter*, vol. 62, no. 10, pp. 6158–6179, Sep. 2000.

[12] M. Boero, A. Pasquarello, J. Sarnthein, and R. Car, "Structure and hyperfine parameters of E'_1 centers in α-quartz and in vitreous SiO_2," *Phys. Rev. Lett.*, vol. 78, no. 5, pp. 887–890, Feb. 1997.

[13] Z. Y. Lu, C. J. Nicklaw, D. M. Fleetwood, R. D. Schrimpf, and S. T. Pantelides, "Structure, properties, and dynamics of oxygen vacancies in amorphous SiO_2," *Phys. Rev. Lett.*, vol. 89, no. 28, p. 285 505, Dec. 2002.

[14] T. Bakos, S. N. Rashkeev, and S. T. Pantelides, "Reactions and diffusion of water and oxygen molecules in amorphous SiO_2," *Phys. Rev. Lett.*, vol. 88, no. 5, p. 055 508, Feb. 2002.

[15] B. W. H. van Beest, G. J. Kramer, and R. A. van Santen, "Force fields for silicas and aluminophosphates based on *ab initio* calculations," *Phys. Rev. Lett.*, vol. 64, no. 16, pp. 1955–1958, Apr. 1990.

[16] P. Vashishta, R. K. Kalia, J. P. Rino, and I. Ebbsjö, "Interaction potential for SiO_2: A molecular-dynamics study of structural correlations," *Phys. Rev. B, Condens. Matter*, vol. 41, no. 17, pp. 12 197–12 209, Jun. 1990.

[17] R. M. Van Ginhoven, H. Jónsson, and L. R. Corrales, "Silica glass structure generation for *ab initio* calculations using small samples of amorphous silica," *Phys. Rev. B, Condens. Matter*, vol. 71, no. 2, p. 024 208, Jan. 2005.

[18] J. Sarnthein, A. Pasquarello, and R. Car, "Structural and electronic properties of liquid and amorphous SiO_2: An *ab initio* molecular dynamics study," *Phys. Rev. Lett.*, vol. 74, no. 23, pp. 4682–4685, Jun. 1995.

[19] G. Kresse and J. Hafner, "*Ab initio* molecular dynamics for liquid metals," *Phys. Rev. B, Condens. Matter*, vol. 47, no. 1, pp. 558–561, Jan. 1993.

[20] G. Kresse and J. Hafner, "*Ab initio* molecular-dynamics simulation of the liquid-metal-amorphous-semiconductor transition in germanium," *Phys. Rev. B, Condens. Matter*, vol. 49, no. 20, pp. 14 251–14 269, May 1994.

[21] G. Kresse and D. Furthmüller, "Efficient iterative schemes for *ab initio* total-energy calculations using a plane-wave basis set," *Phys. Rev. B, Condens. Matter*, vol. 54, no. 16, pp. 11 169–11 186, Oct. 1996.

[22] G. Kresse and D. Furthmüller, "Efficiency of ab-initio total energy calculations for metals and semiconductors using a plane-wave basis set," *Comput. Mater. Sci.*, vol. 6, no. 1, pp. 15–50, Jul. 1996.

[23] G. Kresse and D. Joubert, "From ultrasoft pseudopotentials to the projector augmented-wave method," *Phys. Rev. B, Condens. Matter*, vol. 59, no. 3, pp. 1758–1775, Jan. 1999.

Authorized licensed use limited to: Universitatsbibliothek der TU Wien. Downloaded on December 9, 2008 at 08:13 from IEEE Xplore. Restrictions apply.

[24] S. T. Pantelides, S. N. Rashkeev, R. Buczko, D. M. Fleetwood, and R. D. Schrimpf, "Reactions of hydrogen with Si-SiO_2 interfaces," *IEEE Trans. Nucl. Sci.*, vol. 47, no. 6, pp. 2262–2268, Dec. 2000.

[25] F. Giustino and A. Pasquarello, "Electronic and dielectric properties of a suboxide interlayer at the silicon-oxide interface in MOS devices," *Surf. Sci.*, vol. 586, no. 1–3, pp. 183–191, Jul. 2005.

[26] J. F. Conley and P. M. Lenahan, "Room temperature reactions involving silicon dangling bond centers and molecular hydrogen in amorphous SiO_2 thin films on silicon," *IEEE Trans. Nucl. Sci.*, vol. 39, no. 6, pp. 2186–2191, Dec. 1992.

[27] J. F. Zhang, C. Z. Zhao, A. H. Chen, G. Groeseneken, and R. Degraeve, "Hole traps in silicon dioxides—Part I: Properties," *IEEE Trans. Electron Devices*, vol. 51, no. 8, pp. 1267–1273, Aug. 2004.

[28] A. J. Lelis, H. E. Boesch, T. R. Oldham, and F. B. McLean, "Reversibility of trapped hole annealing," *IEEE Trans. Nucl. Sci.*, vol. 35, no. 6, pp. 1186–1191, Dec. 1988.

[29] J. Godet and A. Pasquarello, "*Ab initio* study of charged states of H in amorphous SiO_2," *Microelectron. Eng.*, vol. 80, no. 1, pp. 288–291, Jun. 2005.

[30] P. E. Bunson, M. Di Ventra, S. T. Pantelides, R. D. Schrimpf, and K. F. Galloway, "*Ab initio* calculations of H^+ energetics in SiO_2: Implications for transport," *IEEE Trans. Nucl. Sci.*, vol. 46, no. 6, pp. 1568–1573, Dec. 1999.

[31] A. Yokozawa and Y. Miyamoto, "First-principles calculations for charged states of hydrogen atoms in SiO_2," *Phys. Rev. B, Condens. Matter*, vol. 55, no. 20, pp. 13 783–13 788, May 1997.

[32] T. L. Tewksbury, "Relaxation effects in MOS devices due to tunneling exchange with near-interface oxide traps," Ph.D. dissertation, MIT, Cambridge, MA, 1992.

[33] L. B. Freeman and W. E. Dahlke, "Theory of tunneling into interface states," *Solid State Electron.*, vol. 13, no. 11, pp. 1483–1503, Nov. 1970.

[34] M. Karner, A. Gehring, S. Holzer, M. Pourfath, M. Wagner, W. Gös, M. Vasicek, O. Baumgartner, C. Kernstock, K. Schnass, G. Zeiler, T. Grasser, H. Kosina, and S. Selberherr, "A multi-purpose Schrödinger-Poisson solver for TCAD applications," *J. Comput. Electron.*, vol. 6, no. 1–3, pp. 179–182, Sep. 2007.

Wolfgang Goes was born in Vienna, Austria, in 1979. He received the Dipl.Ing. degree in technical physics from Technische Universität Wien, Wien, Austria, in 2005, where he has been working toward the Ph.D. degree in the Christian Doppler Laboratory for TCAD in Microelectronics, Institute for Microelectronics since 2006. His diploma thesis addressed grain boundaries in back contact solar cells.

In 2007, he was a Visitor at the Department of Physics and Astronomy, Vanderbilt University, Nashville, TN. His current scientific interests include first-principle simulations of the chemical processes involved in NBTI and HCI, modeling of tunneling and charge trapping in dielectrics, and reliability issues in general.

Markus Karner was born in Vienna, Austria, in 1979. He received the Dipl.Ing. degree in electrical engineering from Technische Universität Wien (TU Wien), Wien, Austria, in 2004.

He has been with the Christian Doppler Laboratory for TCAD in Microelectronics, Institute for Microelectronics, TU Wien, since November 2004, where he was involved in several European and national projects. Since June 2007, he has been the Head of Global TCAD Solutions, Vienna. His scientific interests include modeling and simulation of optical devices as well as modeling of quantum effects in device simulation.

Viktor Sverdlov received the M.S. and Ph.D. degrees in physics from the St. Petersburg State University, St. Petersburg, Russia, in 1985 and 1989, respectively.

From 1989 to 1999, he was a Staff Research Scientist with the V. A. Fock Institute of Physics, St. Petersburg State University. During this time, he held visiting research positions at several European research centers and universities: ICTP (Italy, 1993), University of Geneva (Geneva, Switzerland, 1993–1994), University of Oulu (Oulu, Finland, 1995), Helsinki University of Technology (Espoo, Finland, 1996–1998), Free University of Berlin (Berlin, Germany, 1997), and NORDITA (Copenhagen, Denmark, 1998). In 1999, he was a Staff Research Scientist with the State University of New York, Stony Brook. He has been with the Institute for Microelectronics, Technische Universität Wien, Wien, Austria, since 2004. His scientific interests include device simulation, computational physics, solid-state physics, and nanoelectronics.

Tibor Grasser (M'05–SM'05) was born in Vienna, Austria, in 1970. He received the Dipl.Ing. degree in communications engineering, the Ph.D. degree in technical sciences, and the Venia Docendi degree in microelectronics from the Technische Universität Wien (TU Wien), Wien, Austria, in 1995, 1999, and 2002, respectively.

He is currently an Associate Professor with the Institute for Microelectronics, TU Wien. Since 1997, he has headed the Minimos-NT development group, working on the successor of the highly successful MiniMOS program. He was a Visiting Research Engineer for Hitachi Ltd., Tokyo, Japan, and for the Alpha Development Group, Compaq Computer Corporation, Shrewsbury, MA. Since 2003, he has been the Head of the Christian Doppler Laboratory for TCAD in Microelectronics, an industry-funded research group embedded in the Institute for Microelectronics. He is the coauthor or author of over 200 articles in scientific books, journals, and conference proceedings, and is the editor of a book on advanced device simulation. His current scientific interests include circuit and device simulation, device modeling, and reliability issues.

Dr. Grasser has been involved in the program committees of conferences such as SISPAD, IWCE, ESSDERC, IRPS, IIRW, and ISDRS. He was also a Chairman of SISPAD 2007.

Authorized licensed use limited to: Universitatsbibliothek der TU Wien. Downloaded on December 9, 2008 at 08:13 from IEEE Xplore. Restrictions apply.